
Can we Agree? ON THE RASHŌMON EFFECT AND THE RELIABILITY OF POST-HOC EXPLAINABLE AI

A PREPRINT

Clément Poiret ^{1,2,3,4}, Antoine Grigis ³, Justin Thomas², and Marion Noulhiane ^{1,3,4*}

¹UNIACT, NeuroSpin, CEA Paris-Saclay, Frederic Joliot Institute, Gif-sur-Yvette, France

²Department of Research and Development, Caminov, Paris, France

³NeuroSpin, CEA Paris-Saclay, Frederic Joliot Institute, Gif-sur-Yvette, France

⁴InDEV, NeuroDiderot, Université Paris Cité, Inserm, Paris, France

August 15, 2023

ABSTRACT

The Rashōmon effect poses challenges for deriving reliable knowledge from machine learning models. This study examined the influence of sample size on explanations from models in a Rashōmon set using SHAP. Experiments on 5 public datasets showed that explanations gradually converged as the sample size increased. Explanations from <128 samples exhibited high variability, limiting reliable knowledge extraction. However, agreement between models improved with more data, allowing for consensus. Bagging ensembles often had higher agreement. The results provide guidance on sufficient data to trust explanations. Variability at low samples suggests that conclusions may be unreliable without validation. Further work is needed with more model types, data domains, and explanation methods. Testing convergence in neural networks and with model-specific explanation methods would be impactful. The approaches explored here point towards principled techniques for eliciting knowledge from ambiguous models.

Keywords XAI · Interpretability · Explanations Robustness · Sample size · SHAP

1 Introduction

In recent years, the widespread integration of AI-powered systems in various domains has highlighted the need for increased transparency and trust in these complex models. Explainable AI (XAI) methodologies have emerged as a means to address this need by providing insights into model training and clarifying predictions through post hoc explanations. As these systems become more integrated into our daily lives and are employed in critical domains such as healthcare (e.g. [1, 2]) and cybersecurity (e.g. [3]), it is crucial to understand the basis of their decision-making processes. By unraveling the inner workings of these complex models, we can ascertain whether their conclusions are based on genuine features or merely rely on spurious correlations and shortcuts. In addition, ethical considerations play a role in the adoption and deployment of these AI systems. As they become increasingly sophisticated, it is essential to ensure that their decision-making processes are in line with ethical guidelines and do not follow biases or discriminate against certain individuals or communities. Explainable AI methodologies, such as

the post hoc explanations provided by XAI techniques, offer a means of scrutinizing and mitigate potential biases and ethical concerns. By shedding light on the decision-making process and revealing the factors that contribute to predictions, XAI not only provides accountability, but also empowers stakeholders to address and rectify any biases or ethical issues that may arise. Beyond ethical concerns, if these models outperform human experts on key metrics, illuminating the black box could lead to new findings that might enhance expertise, expand knowledge, or spark new research ideas.

While there is an active research field dedicated to building explainable models out-of-the-box, those models are not yet widely available or as effective as state-of-the-art black-box models in some domains. Therefore, this current work will focus solely on post-hoc explanations: methods that will link a model's prediction to contextual information. Unfortunately, multiple models can perform very well on a given task, but there is no guarantee on their use of similar features to construct their prediction. Multiple models can

*correspondence: marion.noulhiane@cea.fr

base their predictions on multiple set of different features, an effect named “the Rashōmon Effect”

1.1 Explainable AI: a Practical Overview

Although interpretability and explainability may be used interchangeably, interpretability refers to the ability to understand the internal workings and mechanisms of a model, whereas explainability, on which this work will focus, refers to the capacity to provide explanations for the model’s predictions or decisions in a way that can be understood by humans. However, as Del Giudice et al., (2022) previously described [4], there exists a Prediction-Explanation Fallacy. It arises when one employs prediction-optimized models for explanatory purposes, without taking into account the delicate balance between explanation and prediction. On the one hand, of the spectrum lie interpretable models, which are either unrealistically simplistic or complex to deploy in real-world situations. On the other hand, the models employ excessively complex structures that are almost impossible to interpret (Figure 1). Thus, if explainability can come from models with built-in explanation mechanisms (e.g. ref), the easiest approach comes from post hoc explanation methods, as they allow the explanation of any given model, for any given task. Finally, the objectives of explainability are (i) to provide information on the training or generalization of a specific model, or (ii) to clarify its predictions by explaining them in terms of the input of the model [5]. By addressing the question of “*why did this model make this particular prediction?*”, XAI generates a set of features that highlight distinct patterns present in a model’s internal representation of a phenomenon.

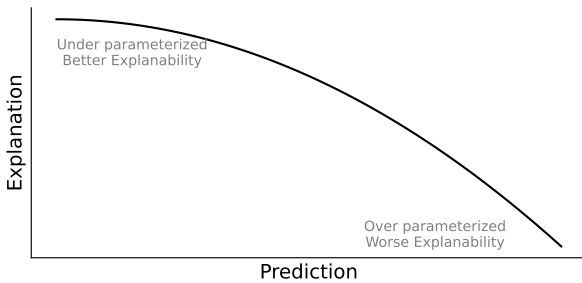


Figure 1: Usual Perception of the Prediction-Explanation trade-off. The prediction-explanation trade-off illustrates the difficulty behind XAI. The more complex a model is, the more predictive power it has, but its use of highly complex structures render its interpretability nearly intractable.

Post-hoc explainability encompasses two main approaches: model-specific and model-agnostic methods. Model-specific methods are tailored to a specific type of model and provide insight into its internal workings. For example, attention maps (e.g. ref) highlight the important regions in an image that contribute to the model’s prediction, while GradCAM (e.g. [6]) visualizes the regions that are crucial for a specific class. On the other hand, model-agnostic

methods are applicable to any model and focus on explaining predictions without accessing internal information such as weights or architecture [7]. SHAP (for SHapley Additive exPlanations) [8] - the most popular method of this kind - uses Shapley values to attribute the importance of each input feature in making the final prediction. For example, in an image classification task, SHAP can identify the pixels that contribute the most to the predicted class. Shapley values are a way to fairly distribute the “credit” for a particular outcome among the different factors that contributed to it. In the context of Machine and Deep Learning, “credit” refers to the importance of each input feature (e.g. pixels in an image) in making the final prediction. SHAP computes the Shapley value for each feature by considering all possible combinations of features and measuring the change in prediction.

In addition to the increase in trust and transparency, explaining a model gives the possibility of detecting inconsistencies in its modeling quality. Some models may demonstrate equivalent predictive accuracy, but their biases may be distinct, implying the “Rashōmon effect”, — i.e. conflicting interpretations of the underlying phenomenon [9].

1.2 On the Rashōmon Effect

The tension between prediction and explanation is correlated to the Rashōmon Effect. According to Anderson (2016), the Rashōmon Effect “is the naming of an epistemological framework—or ways of thinking, knowing, and remembering—required for understanding the complex and ambiguous on both the small and large scale” [10]. It originates from a Japanese film of the same name, by Akira Kurosawa, which portrays a crime from four different perspectives, each with a different interpretation of the event caused by the subjectivity of human perception and memory. Thus, Breiman (2001) imported the concept into statistics and Machine Learning, where the concept refers to the phenomenon in which different near-optimal models trained on the same task may actually base their prediction on different sets of features [9]. Different models that perform similarly may have different underlying structures and assumptions.

Those models fall into what we call a Rashōmon set: a set of models showing the same predictive power, i.e., models whose training loss is below a specific threshold. Given a loss function L and a model class F , the Rashōmon set R can be written as [11]:

$$R(F, f^*, \epsilon) = \{f \in F \text{ such that } L(f) \leq L(f^*) + \epsilon\}$$

where f^* is an optimal model, ϵ is a threshold named the Rashōmon parameter. While multiple models can be found at $\epsilon = 0$, we usually use an ϵ -level set where $\epsilon > 0$ [12] because a low ϵ could result in an empty set. It has to be noted that computing the Rashōmon set is NP-hard and requires brute-force methods by sampling the hypothesis space [11].

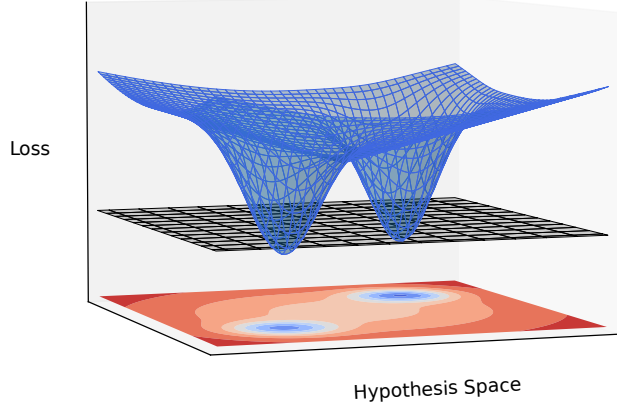


Figure 2: A simplified example of a Rashōmon set in a two-dimensional hypothesis space. The loss of each model in the space is in blue, while the black plan represents the value of the Rashōmon parameter, ϵ . As a result, the Rashōmon set is illustrated in blue in the projection at the bottom of the figure.

Let H be the hypothesis space that contains all possible models M , and let f_1 and f_2 be two near-optimal models in $R(F, f^*, \epsilon)$ of H . The Rashōmon Effect refers to the phenomenon where f_1 and f_2 produce similar predictions on the same input x , despite showing different feature importances. Formally, with w_1 and w_2 be the feature importances of f_1 and f_2 respectively, let r_1 and r_2 be the ranks of each feature. Intuitively, we can say that we observe a Rashōmon effect when:

$$r_1 \neq r_2$$

The Rashōmon Effect, in this case, can be problematic because it can lead to different interpretations of the same dataset and make it difficult to identify the most important features for a given task, or even to derive reliable knowledge from this interpretation.

1.3 Finding a Consensus

As formulated by Teney et al. (2022), predicting is not understanding [13]. The presence of the Rashōmon effect can be seen as a manifestation of underspecification, where a model fails to capture all the underlying patterns in the data accurately. To address this issue, Teney et al. propose training multiple models that are compatible with the data. Del Giudice (2022) suggests several ways to mitigate this problem, notably: (i) seeking consensus among models with different assumptions or biases, and (ii) noting that the severity of this effect tends to decrease when working with larger datasets [4].

Thus, we hypothesize that:

1. if computing the Rashōmon set without brute force is challenging, it is still possible to identify models that belong to the set,

2. the robustness against small input perturbations increases as the sample size grows,
3. the agreement among explanations from diverse models in the Rashōmon set converges, allowing for a consensus when the sample size is sufficiently large.

To further enhance the exploration of the Rashōmon effect, we included a bootstrap aggregation (bagging) strategy, a common method that enhances overall performance by alleviating fluctuations in predictions from multiple models, as we can suppose that they do so also by minimizing the variability of feature importances. To investigate the said hypothesis, the work has been organized into three main contributions on five distinct public datasets.

1. we proposed a methodology to assess an intra-model agreement, in which the explainability is disturbed by a varying input dataset through cross-validation,
2. we proposed a methodology to assess an inter-model agreement, and its convergence toward a consensus,
3. we analyzed the behavior of a bagging strategy to assess its behavior with respect to intra- and inter-model agreement.

The intent of this paper is not to benchmark explanation methods, but instead presents a novel approach to evaluating the robustness of explanations, notably with respect to sample size. The general goal of the present work is to propose a new framework for computing explanations of machine learning models (Figure 3). Its aim is to emphasize the fact that explaining a model is not enough, but we need to assess the convergence and robustness of feature importances.

2 Methodology

The method (Figure 3) can be divided into four parts: (i) a pre-selection of models based on their performances on the training set (Table 2) followed by their hyperparameter tuning to ensure we ended up in a Rashōmon set; (ii) a 10-fold cross-validation on subsets of the training set with varying size of each model, to ensure that the models are generalizing well; (iii) a bagging strategy on all the selected models, which is a technique that combines the predictions of multiple models to improve the overall accuracy; and (iv) an inference on a holdout test set followed by an explanation using the SHAP methodology. All training, inference, and explanation steps are summarized in algorithm 1. As sample size might have an impact on hyperparameters, we conducted a simple hyperparameter tuning using a random search strategy for each instance of a model, to ensure that the best hyperparameters are chosen for each model.

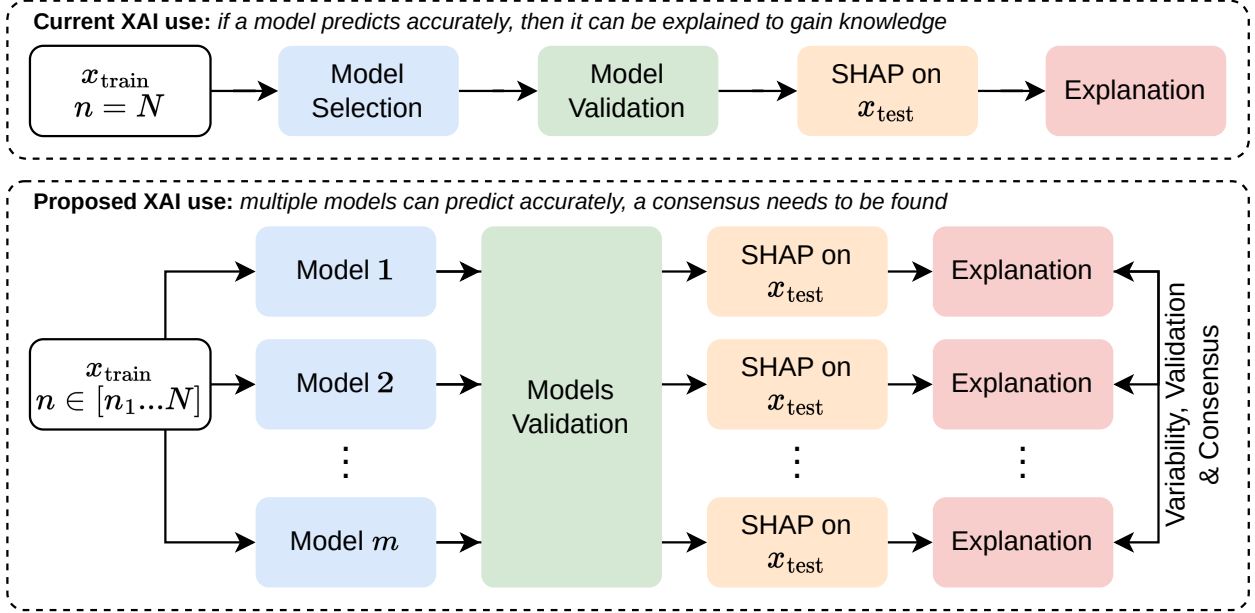


Figure 3: Proposed framework for enhancing explainability through model validation and consensus finding. It illustrates the proposed framework to improve the reliability of explanations from machine learning models. In contrast to the typical use of XAI methods where a single predictive model is explained, the proposed approach first validates multiple high-performing models on a dataset. SHAP explanations are generated for each model in the validation stage. The resulting explanations are then analyzed to find consensus and reduce variability, leading to more trustworthy explanations.

2.1 Datasets

To test our hypothesis under various realistic conditions, we conducted our experiments on five datasets (Table 1, of various sizes, dimensionality, and with or without class imbalance. Most of them come from the OpenXAI framework, an open initiative for the robust and repeatable evaluation of XAI methodologies [14].

2.2 Exploring the Rashōmon Set

The first step of this methodology is to select the models that we will explain. As the exploration of the Rashōmon set is NP-hard, its space has been divided into categories of models M (see Table 2). Using the PyCaret library [19], each of these models has been benchmarked with multiple configurations using 10-fold cross-validation, and the three configurations with the highest Cohen’s Kappa coefficient have been selected. The Cohen’s Kappa coefficient [20] is a statistical measure of the interrater agreement taking into account the possibility of agreement occurring by chance. This is particularly important in cases where the classes are imbalanced. In addition to these top 3 models, a bagging strategy has been implemented by combining the predictions of the aforementioned models to further improve the overall comparison.

2.3 Shapley Additive Explanations (SHAP)

After model selection and training, the core of our hypothesis relies on feature importances that have to be comparable across all models. As all datasets are already given by the original authors as separate train and a test sets, each model inferred on the latter. Each model state - i.e. each cross-validation step at each sample size - went through the SHAP pipeline [21]. We chose the SHAP method for its ease of use, widespread adoption, and its axiomatic superiority to its counterpart. Shapley-based explanation methods provide a way to assign each feature an importance in a model-agnostic way [21], allowing the comparison between very different models that could have been previously selected. It has to be noted that, while SHAP is a methodological choice, the method we introduce could have been used with any other explanation framework. Following the definition of [22], let $\phi_{f_i}^{SHAP}$ be the SHAP values obtained from a machine learning model f_i , for a set of n instances and their labels y in a dataset X of K features. In simpler terms, SHAP values are used to explain predictions made by a model at an individual level. Transitioning from the individual level to the population level can be achieved by taking the mean of the absolute values of the vector $\phi_{f_i}^{SHAP}$ across all instances:

$$\frac{1}{N} \sum_{n=1}^N |\phi_{f_i}^{SHAP}_n|$$

Dataset	Short name	N	N Features	Balanced
Framingham Heart study [15]	Framingham	4240	16	No
German Credit [16]	German	1000	20	No
Pima-Indians Diabetes [17]	Diabetes	768	9	No
COMPAS [18]	Compas	18876	7	No
Student [14]	Student	100	30	Yes

Table 1: Datasets used to study the Rashōmon effect.

Algorithm 1 Model Selection and Explanations

Input: x_{train}, x_{test} (training and test sets)
Output: sim_{intra}, sim_{inter} (similarities between explanations)

```

1: procedure SELECT( $M$ )
2:    $r = []$  ▷ Array of Kappa scores
3:   for  $f \in M$  do
4:     TRAIN( $f, x_{train}$ )
5:      $\hat{y} = f(x_{test})$ 
6:      $\mathcal{K} = \text{Kappa}(\hat{y}, y)$ 
7:      $r.append(\mathcal{K})$ 
8:   end for
9:    $top_3 = \text{Sort}(\text{Rank}(r))[:, -1][3]$ 
10: end procedure
11: procedure EXPLAIN( $top_3$ )
12:    $S = \{2^4, 2^5, \dots, N\}$  ▷ Varying sample sizes
13:    $\Phi = []$  ▷ Array of explanations
14:   for  $s \in S$  do
15:      $x = x_{train}[:, s]$ 
16:     for  $f \in top_3$  do ▷ Repeated as 10-Fold CV
17:       TRAIN( $f, x$ )
18:        $\hat{y} = f(x_{test})$ 
19:        $\phi_f^{SHAP} = \text{EXPLAIN}(\hat{y})$ 
20:        $\Phi.append(\phi_f^{SHAP})$ 
21:     end for
22:   end for
23:    $sim_{intra} = \text{similarity}(\Phi|s)$  ▷ For each model,
computes the similarity between cross-validation folds
24:    $sim_{inter} = \text{similarity}(\Phi|f)$  ▷ For each sample
size, computes the similarity between all the models
25: end procedure

```

2.4 Evaluating the similarity between multiple explanations

As our main goals were to compare the SHAP values given by (i) the same models with variations in the training set induced by cross-validation, and (ii) different near-optimal models on the same training set, we defined two metrics. First, since not all features may be of interest, we used a top_j similarity as introduced in [23]. Then, we used a weighted cosine similarity, which allows us to compare the similarity between multiple vectors while taking into account that features that are not important are possibly randomly ranked by a given model f_i .

Model	Acronym	Linearity
Logistic Regression	lr	Linear
Linear Discriminant analysis	lda	Linear
Ridge	ridge	Linear
Gaussian Naive Bayes	nb	Linear
Singular Vector Machine	svm	Linear
Singular Vector Machine (RBF)	rbfsvm	Non-linear
Decision Tree	dt	Non-linear
Quadratic Discriminant analysis	qda	Non-linear
Random Forest	rf	Non-linear
AdaBoost	ada	Non-linear
Extra Trees	et	Non-linear
Gradient Boosting	gbc	Non-linear
K-Nearest Neighbors	knn	Non-linear
Gaussian Process	gp	Non-linear
CatBoost	catboost	Non-linear
LightGBM	lightgbm	Non-linear
XGBoost	xgboost	Non-linear

Table 2: List of all models included in our experiments. For each dataset, all models are trained and tuned, and the best ones are kept for further analysis.

2.4.1 Metrics

top_j Similarity

The top_j similarity metric is a useful tool for comparing the similarity between two sets of features selected by different models. This metric is based on the idea that not all features may be of interest, and therefore, we can focus on the top j features selected by each model. When comparing the overlap between these top j features, we can obtain a measure of similarity between the two models. This metric is particularly useful when comparing models with different feature selection methods or when only a subset of features is relevant to the problem at hand. The top_j similarity metric is a simple, yet effective way to compare the interpretability of different machine learning models and can provide valuable insight into the behavior of these models. To begin with, let us define the ranking function R that maps the SHAP values to the ranked features as follows:

$$R(\phi_{f_i}^{SHAP} = \text{argsort}(|\phi_{f_i}^{SHAP}|)[::-1][:j]) \quad (1)$$

where $\text{argsort}(a)$ returns the indices that would sort the array a in ascending order, and the indexing operation $[:, -1]$ reverses the order of the sorted indices to obtain the

descending order. The final indexing operation $[: j]$ selects the top j indices based on this ranking.

Using this ranking function, we can obtain the sets of top j features selected by models f_1 and f_2 for the n -th instance as $S_n^{f_1} = R(\phi_n^{SHAP_{f_1}})$ and $S_n^{f_2} = R(\phi_n^{SHAP_{f_2}})$. The top_j similarity metric is the ratio of the average number of common features between the two models and j , where j is the number of features selected. Thus, the top_j similarity metric can be expressed as:

$$top_j \text{ similarity} = \frac{1}{j} \sum_{i=1}^j \frac{|S_i^{f_1} \cap S_i^{f_2}|}{|S_i^{f_2}|}$$

Here, the numerator represents the number of common features between the two models, and the denominator represents the number of features selected by the second model. As we compare M models, the final metric top_j^M computes the mean top_j similarity between all possible combinations of two different models using their respective SHAP values, such as:

$$top_j^M \text{ similarity} = \frac{1}{\binom{M}{2}} \sum_{a,b \in \binom{[1,M]}{2}} top_j \text{ similarity}(a,b) \quad (2)$$

where $\binom{M}{2}$ is the number of possible combinations of two different models, and $\binom{[1,M]}{2}$ is the set of all such combinations.

Weighted Cosine Similarity

We introduced the weighted cosine similarity as a useful metric to compare similarity between multiple vectors while considering that features that are not important are possibly randomly ranked by a given model f_i . First, with K features, we compute the mean absolute SHAP value for each feature k across all samples as:

$$mas_k = \frac{1}{K} \sum_{k=1}^K |\phi_{f_i,k}^{SHAP}|$$

Then, we compute the weighted SHAP values for each feature k as:

$$w_{f_i,k} = |\phi_{f_i,k}^{SHAP}| \cdot mas_k$$

where $k \in \{1, K\}$. Let us define the weighted cosine similarity $wcossim$ between models f_1 and f_2 such as:

$$wcossim(w_{f_1}, w_{f_2}) = \frac{w_{f_1} \cdot w_{f_2}}{\|w_{f_1}\|_2 \|w_{f_2}\|_2}$$

where \cdot denotes the dot product and $\|\cdot\|_2$ denotes the Euclidean norm. Similarly to top_j similarity, we can finally define $wcossim^m$ as the weighted cosine similarity between all combinations of two different models:

$$wcossim^M = \frac{1}{\binom{m}{2}} \sum_{a,b \in \binom{[1,M]}{2}} wcossim(a,b) \quad (3)$$

We used the weighted cosine similarity to compare the similarity of models' SHAP values while accounting for the randomness of unimportant feature ranking.

2.5 Assessing the convergence towards a near-optimal consensus

The mean of the absolute SHAP values for the largest sample size N available from all models f_i can be expressed as:

$$\bar{\phi}_{consensus}^{SHAP} = \frac{1}{MN} \sum_{i=1}^M \sum_{j=1}^N |\phi_{f_i,j}^{SHAP}| \quad (4)$$

where $\bar{\phi}_{consensus}^{SHAP}$ represents the mean absolute SHAP values for the consensus of all models, M is the total number of models, N represents the largest sample size available across all models, and $|\phi_{f_i,j}^{SHAP}|$ represents the absolute SHAP value for the j -th instance of the i -th model. This formulation calculates the mean of the absolute SHAP values across all instances and models for the largest available sample size N , providing a baseline for comparison with the evolution of the explanations of individual models over time.

2.6 Statistical Analysis

To assess the intra-model agreement, we used Spearman correlations between sample sizes and the weighted cosine similarities of each individual model on the SHAP values computed at each step of the cross-validation. Spearman correlations are used to account for the monotonic nonlinear nature of the relationship. A similar analysis is performed for the inter-model analysis, where we computed Spearman correlations between sample sizes and weighted cosine similarities between individual models and the consensus $\bar{\phi}_{consensus}^{SHAP}$. To account for multiple comparisons, p -values are corrected using the Benjamini-Hochberg false discovery rate (FDR) [24].

3 Results

Having selected the top three models that maximize the Kappa coefficient on the training set, we then computed their performances on the test set. Subsequently, we compared both their internal variability (i.e., the variability caused by the cross-validation) and their overall relative variability (i.e., the variability caused by a switch of near-optimal models).

3.1 Models performances

We implemented a 10-fold cross-validation strategy to assess the accuracy (ACC), F1, and Matthews correlation

coefficients (MCC) of various models on the Framingham, German, Diabetes, Compas, and Student datasets, the results of which are illustrated in Table 3. The findings showed the existence of a Rashōmon set for the Framingham, Compas, Diabetes, and Student datasets, where the precision, F1 score, and MCC of the proposed models were similar. An examination of the learning curve revealed that most of the models reached a convergence state for the Framingham, Diabetes, Compas, and Student datasets, as shown in Figure 4. Interestingly, it can be noted that none of the models successfully converged on the German dataset, which is characterized by high dimensionality and exhibits a pronounced class imbalance, in contrast to the Student dataset where optimal performance levels were achieved early in the learning progression, as depicted in Figure 4.

	ACC	F1	MCC
A.			
baseline	0.663 ±0.001	0.231 ±0.001	0.200 ±0.002
nb	0.833 ±0.001	0.268 ±0.002	0.196 ±0.002
qda	0.828 ±0.006	0.318 ±0.007	0.228 ±0.002
lda	0.808 ±0.001	0.354 ±0.001	0.242 ±0.001
bagging	0.841 ±0.001	0.24 ±0.004	0.19 ±0.004
B.			
baseline	0.535 ±0.060	0.600 ±0.073	-0.320 ±0.000
gpc	0.595 ±0.001	0.714 ±0.001	0.022 ±0.001
et	0.65 ±0.001	0.783 ±0.001	-0.072 ±0.001
nb	0.5 ±0.000	0.59 ±0.000	-0.005 ±0.000
bagging	0.504 ±0.012	0.603 ±0.019	-0.026 ±0.005
C.			
baseline	0.721 ±0.001	0.581 ±0.001	0.393 ±0.000
rbfsvm	0.759 ±0.003	0.622 ±0.018	0.449 ±0.009
et	0.759 ±0.006	0.622 ±0.028	0.451 ±0.019
gpc	0.739 ±0.001	0.583 ±0.0	0.397 ±0.001
bagging	0.748 ±0.001	0.598 ±0.001	0.418 ±0.003
D.			
baseline	0.850 ±0.000	0.912 ±0.000	0.413 ±0.000
catboost	0.853 ±0.002	0.914 ±0.001	0.432 ±0.010
gbc	0.851 ±0.005	0.913 ±0.003	0.427 ±0.019
ada	0.851 ±0.003	0.913 ±0.002	0.429 ±0.007
bagging	0.854 ±0.001	0.915 ±0.001	0.438 ±0.005
E.			
baseline	0.960 ±0.000	0.947 ±0.002	0.918 ±0.000
xgboost	0.980 ±0.001	0.976 ±0.001	0.959 ±0.001
catboost	1.000 ±0.000	1.000 ±0.000	1.000 ±0.000
dt	0.960 ±0.001	0.947 ±0.001	0.919 ±0.001
bagging	0.980 ±0.001	0.974 ±0.001	0.959 ±0.001

Table 3: Test-set performances of the sampled models on accuracy (ACC), F1, and Matthews Correlation Coefficients (MCC) on the Framingham (A), German (B), Diabetes (C), Compas (D), and Student (E) datasets. Bold results indicate best models. The baseline is a simple logistic regression.

3.1.1 Intra-model agreement

In our analyses of the Compas, Diabetes, and Framingham datasets, we found a significant correlation between sample size and intramodel agreement, as shown in Table 4.

However, this correlation was absent in the context of the Student dataset where, remarkably, even with smaller sample sizes, we recorded great levels of predictive precision and harmony, as evidenced in Table 3. Conversely, the German dataset exhibited persistently poor predictive accuracy throughout our experimental endeavors, a deficiency mirrored in the intra-model agreement. Overall, the top_j similarity demonstrated a propensity for the top_j features to converge toward uniformity, particularly for the bagging models (Figure 5). These models displayed a higher internal agreement on the Framingham, German, and Diabetes datasets. An intriguing insight was the ability to attain a high degree of agreement with smaller samples, a level that initially receded but subsequently increased as the sample size grown.

	p	p_{cor}	r	power
compas	0.000	0.000	0.889	1.000
diabetes	0.025	0.061	0.458	0.635
german	0.664	0.664	0.080	0.072
framingham	0.045	0.075	0.412	0.534
student	0.097	0.122	0.298	0.389

Table 4: Correlation between sample size and intra-model correlation. Results are Spearman correlations between similarities of cross-validation explanations and sample size.

3.1.2 Inter-model agreement and consensus

The outcomes of the convergence towards an optimal consensus is similar to the intramodel agreement. Nearly each individual model converges towards the near-optimal consensus $\bar{\phi}_{consensus}^{SHAP}$ (Table 5 and Table 6), except for the student model, which demonstrates a significantly high level of similarity even for small sample sizes. As for the German model, it follows a U-shaped pattern with respect to the sample size (Figure 6).

	p	p_{cor}	r	power
compas	0.000	0.000	0.766	0.999
diabetes	0.000	0.000	0.862	0.999
german	0.111	0.139	0.334	0.366
framingham	0.000	0.000	0.875	1.000
student	0.654	0.654	-0.096	0.073

Table 5: Correlation between sample size and inter-model correlation convergence towards the best consensus. Results are Spearman correlations between similarities of all models and $\bar{\phi}_{consensus}^{SHAP}$ and sample size.

4 Discussion

The problem of the existence of multiple high-performing models relying on different features — the Rashōmon effect — poses significant challenges to derive reliable knowledge from machine learning systems. In this study,

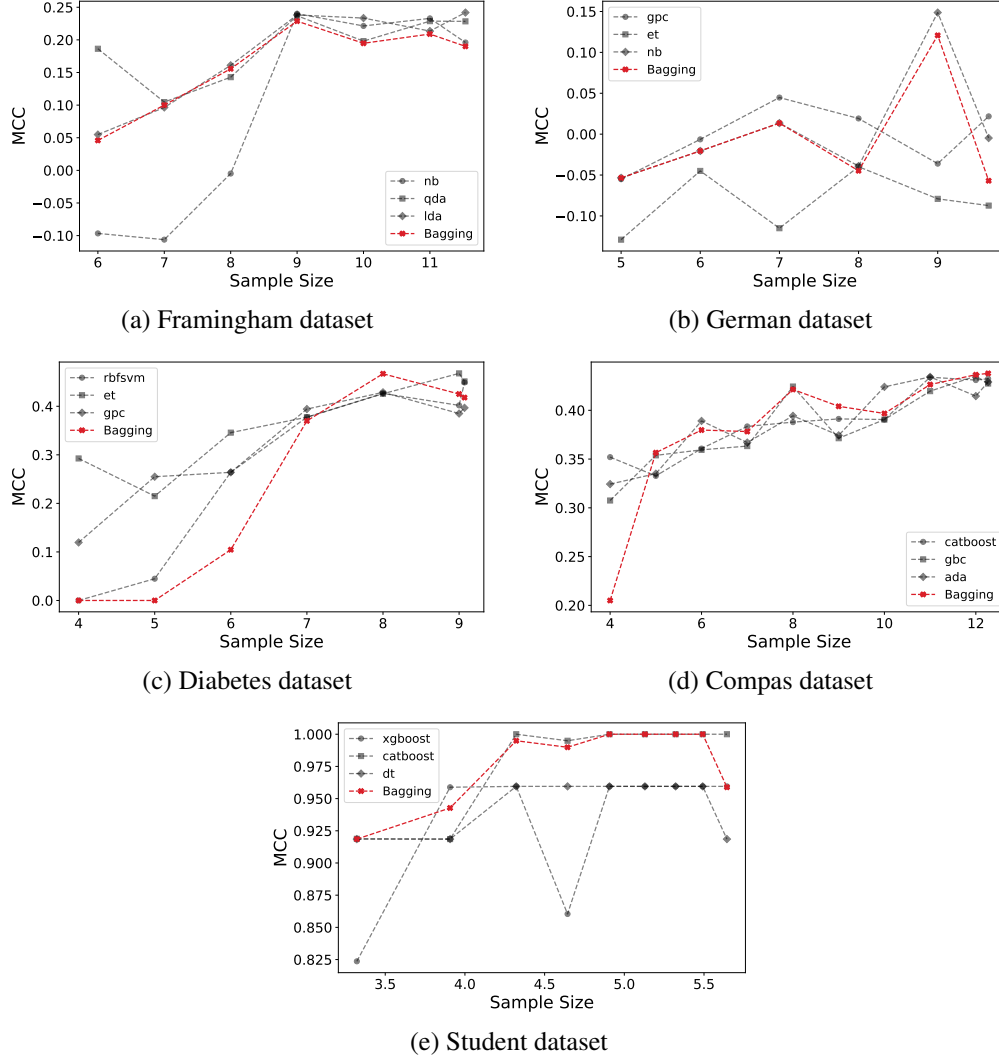


Figure 4: Impact of the sample size on model performance (Matthews Correlation Coefficient, MCC). MCC is computed on the test set during a 10-fold cross-validation. The gray lines represent individual models, and the red line represents the result when a bagging strategy is used on all models. Sample sizes are on a log2 basis.

	p	p_{cor}	r	power
compas	0.067	0.084	0.633	0.483
diabetes	0.000	0.000	1.000	1.000
german	0.037	0.061	0.738	0.604
framingham	0.329	0.329	0.486	0.171
student	0.002	0.005	0.905	0.936

Table 6: Correlation between sample size and bootstrap aggregation convergence towards the best consensus. Results are Spearman correlations between similarities of a bagging strategy of all top_3 models and $\bar{\phi}_{consensus}^{SHAP}$ and sample size.

our aim was to examine the influence of sample size on models within a Rashōmon set using a model-agnostic explainability technique. Our research revolved around

two main aspects: (i) the enhancement of explainability in relation to sample size, and (ii) the convergence of explanations from diverse models in the Rashōmon set, leading to a consensus when the sample size reaches a sufficient size. Additionally, we explored the characteristics of bagging strategies within the same scenarios to gain additional information. The key findings of this study demonstrate the substantial impact of sample size on the reliability and agreement of explanations from machine learning models that exhibit a Rashōmon effect (Table 4, Table 5, and Table 6). Our experiments in five public data sets revealed that explanations derived from subsets with fewer than 128 samples showed high variability in cross-validation, indicating spuriousness (Figure 5 and Figure 6). This effectively limits the actionable knowledge that can be extracted from any single model’s interpretations. However, as the

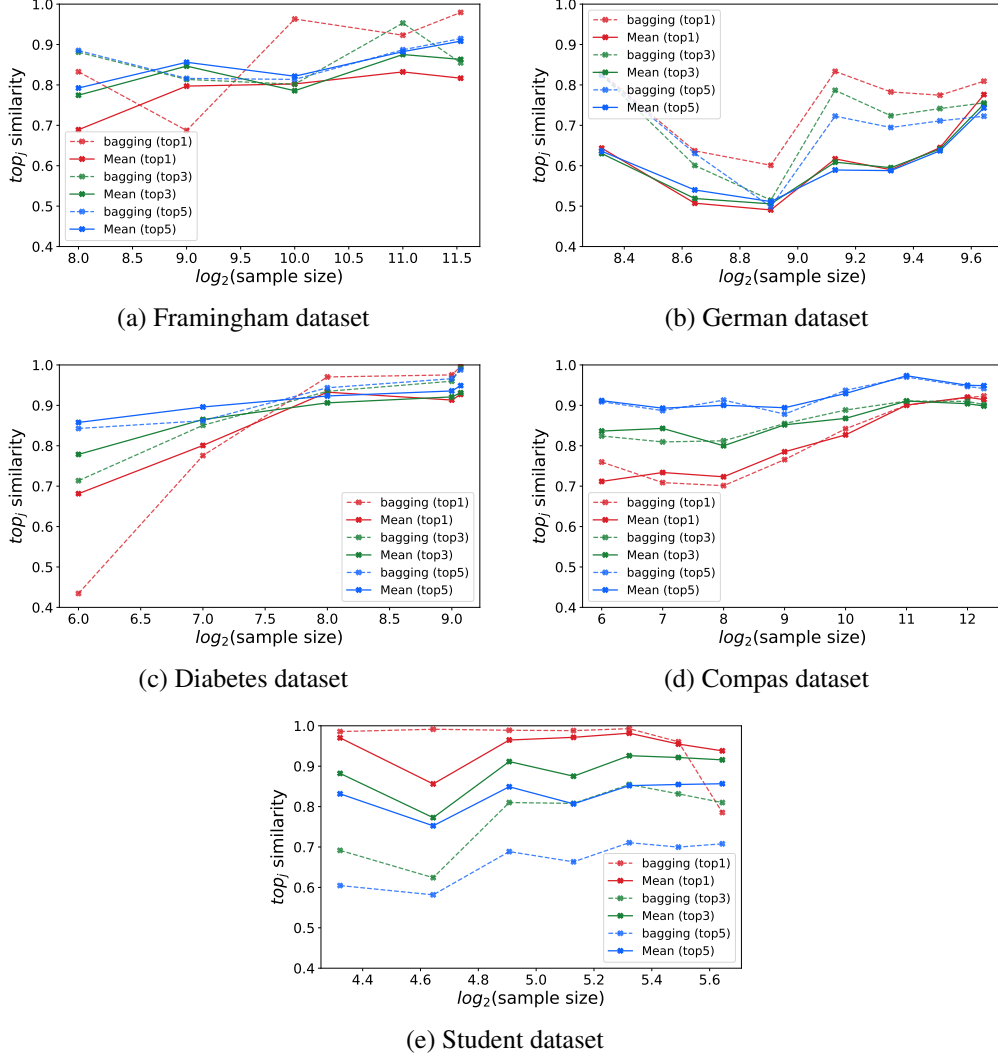


Figure 5: Impact of the sample size on top_j similarity between model explanations. Explanations given for each model are computed using a 10-fold cross-validation. The dashed lines in light colors represent individual models, the solid lines represent the mean top_j for $j = 1$, $j = 3$, and $j = 5$ across all models, and their lighter counterparts represent a bagging strategy on all models.

sample size increased, the variance in similarity diminished and models converged towards a unified explanation.

Our first experiment was primarily devoted to the study of model robustness when the training set is perturbed through cross-validation, a property we named internal agreement. All models, except the one used for the German dataset, demonstrated convergence towards an acceptable level of classification accuracy (Figure 4 and Table 3), while manifesting a strong correlation between sample size and weighted cosine similarity (Table 4). However, it is important to highlight two exceptions. The first pertains to the methodologies employed on the German dataset, which were unable to identify suitable models within the Rashōmon set, implying that no models were successful in determining a valid solution, resulting in a lack of con-

vergence in internal agreement. The second exception is linked to the Student dataset, where convergence was observed remarkably early in the learning trajectory (Figure 4e), indicating that a high degree of internal agreement was achieved at the beginning of the experiment itself. An interesting insight was the nonlinear association between the sample size and the intra-model consensus. At small sample sizes, high similarity could be achieved (Figure 5b) despite a poor predictive capacity (Figure 4b), which subsequently experienced a decline, only to ascend once again with the addition of more data. This aligns with previous research indicating false confidence in underspecified models [25], drawing a parallel to the Dunning-Kruger effect observed in human learning. Although the agreement on the German dataset seems to increase, this suggests that more data is needed to perform our analysis on our dataset.

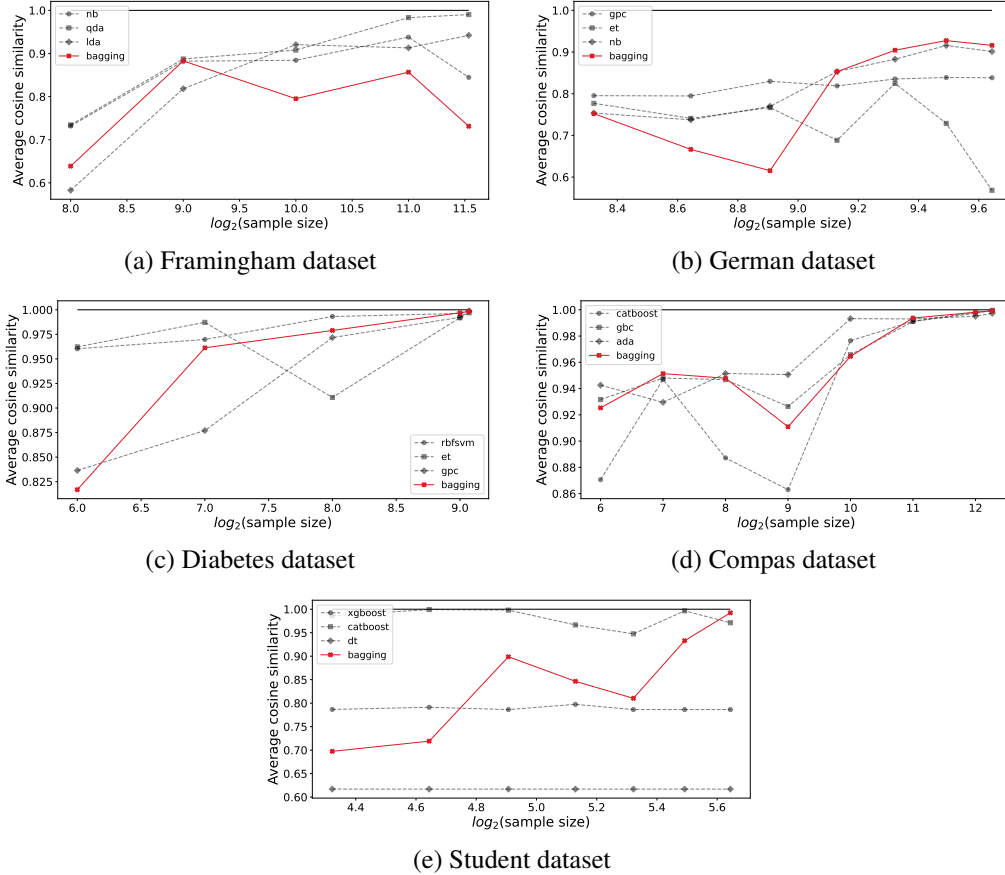


Figure 6: Impact of the convergence of models towards the best consensus available. Explanations given for each model are computed using 10-fold cross-validation. Dashed lines represent individual models; the black line represents the best consensus available (the mean of the absolute SHAP values for the biggest sample size available). The red line represents the result when using a bagging strategy on all models.

The second important point that this experiment highlights is the regular superiority of bagging approaches, where they showed higher internal agreement at large sample sizes for 3 of our 5 datasets (Figure 5), but this was not always the case at low sample sizes, especially for the Diabetes dataset. This first experiment allows us to say that while sample size has a positive impact on a model’s internal agreement, performance is not always correlated to agreement in explanations, highlighting the need to perform additional analysis before the explanation of machine learning models. Moreover, contrary to popular belief, bagging is not always the best strategy — especially at low sample sizes — regarding explainability.

The supplementary experiment engaged in an in-depth exploration concerning the coherence among various models and their convergence towards a near-optimal consensus, — the average explanation of high-performing models at the highest sample size. Once again, we observed a positive correlation between the sample size and the agreement among the high-performance models (Table 5 and Table 6). Analogous to the intra-model agreement, the experiment failed to exhibit any correlation within the Student dataset

due to the previously delineated complications. The convergence of inter-model explanations reaffirms the hypothesis that large datasets attenuate the Rashōmon effect and facilitate reliable knowledge extraction [4]. Despite the fact that the bagging ensembles did not always converged better than the individual models (Figure 6a, c, and d), they converged towards the optimal solution, while some models remained stuck within their respective basins (Figure 6e). This secondary experiment allows the conclusion that the learning process functions herein as a refinement of feature importance, a process whereby an increase in sample size triggers a convergence towards a singular, coherent explanation of the predictions. However, it is interesting to observe the phenomenon that underscores the disparities between a consensus derived from explanations coming from diverse models, and the explanation of a bagging procedure over the exact same models (e.g. Figure 6a). Although it was generally not possible to differentiate between the predictive performance of individual models and the bagging procedure (Figure 4), this research does not offer the means to draw a definitive conclusion about which is superior: should we favor the explanation derived

from an aggregation of multiple models, or a consensus predicated upon the explanations of the individual models? However, the conclusion we can draw is that both were similar for 4 datasets in the 5 we studied, meaning that our method should be appropriate in both cases.

However, there are some limitations to the generalization of these findings. First, this study limited itself to certain types of models, such as linear models or random forests. Testing other complex models, such as neural networks, could reveal different behaviors and challenges. Extending this research to neural network models presents challenges due to their complexity, but also opportunities to mitigate the Rashōmon effect through transfer learning. As shown by [26], different initializations of the same architecture can learn distinct solutions. Transfer learning provides more consistent representations and could align explanations between models, because the learning on the specific task starts in an already nonrandom state. Questions such as “does the surrogate task impact explanations?” or “are explanations found through transfer learning better than those of models trained from scratch?” remain to be answered. Testing the sample size effects shown here in deep learning scenarios with and without transfer learning would be an impactful extension.

Second, while the datasets covered various sizes and domains, more extensive experiments are needed on diverse real-world problems, which could include regression problems. Regarding those datasets, the Student task was definitely too simple for the correct assessment of our methodology, even if it allowed us to draw interesting conclusions. However, the German dataset clearly requested a modified methodology, certainly a dimensionality reduction, such as PCA, or a class-imbalance correction, such as SMOTE. We intentionally chose not to adopt this modified methodology to stay consistent with the other analysis. Also, PCA would have complexified our SHAP workflow as we would have had to interpret its principal components. However, this raises a relevant link between the curse of dimensionality and overconfidence issues in machine learning models as described in other works (e.g. [27]).

Finally, while this study used SHAP, a model-agnostic approach, further research could explore how model-specific explanation methods such as attention maps or Grad-CAM behave in the context of the Rashōmon effect. As model-specific techniques provide insights into a model’s internal representations, they may reveal divergences between architectures that model-agnostic methods cannot access. Comparing the convergence patterns of both approaches could offer additional validation and confidence in the explanations. Furthermore, the evaluation of other post-hoc explanation techniques such as LIME could reveal different insights. For example, LIME perturbs inputs and trains interpretable local models, which may show higher variability at low sample sizes. Testing multiple perturbation and explanation strategies could indicate which are the most robust for reliable explanations from underspecified models.

Despite these constraints, this work has meaningful practical implications. The results suggest that sample sizes below 100 can lead to unreliable explanations that lack consensus between equally performing models. We argue that our methodology provides a kind of power analysis to determine sufficient data to trust explanations. Furthermore, the variability at low sizes indicates that conclusions drawn from small datasets could be spurious and should be validated. In general, these findings can guide machine learning practitioners in selecting appropriate data volumes, models, and explanation techniques for their applications.

Future work should explore ensembles such as bagging for explanation robustness across broader model types, data domains, and explanation methods. Testing the Rashōmon effect in online learning settings where models are continuously retrained would also have a great impact. As interpretations become increasingly critical for trustworthy AI, developing a rigorous understanding of how to evaluate, improve, and trust model explanations remains an essential challenge. The approaches explored here — leveraging sample size, ensembles, consensus-finding, and variability quantification — point towards principled pathways for eliciting knowledge from ambiguous models. This study provides an initial data-driven perspective on this important problem.

5 Conclusion

This study examined how sample size impacts the explainability of models that exhibit Rashōmon effect. Experiments on multiple datasets revealed explanations become more consistent as sample size grows, with variability limiting reliability below 100 samples. Key takeaways for practitioners include: 1) larger data volumes attenuate the Rashōmon effect and improve explanation consensus, 2) explanations derived from limited data may be spurious and require validation, 3) bagging ensembles can enhance agreement between models. Overall, these findings provide guidance on selecting appropriate sample sizes, models, and explanation techniques when interpreting machine learning systems to ensure credible and actionable knowledge.

References

- [1] Andrzej Grzybowski and Piotr Brona. Approval and Certification of Ophthalmic AI Devices in the European Union. *Ophthalmology and Therapy*, 12(2): 633–638, April 2023. ISSN 2193-8245, 2193-6528. doi: 10.1007/s40123-023-00652-w.
- [2] Mohit Pandey, Michael Fernandez, Francesco Gentile, Olexandr Isayev, Alexander Tropsha, Abraham C. Stern, and Artem Cherkasov. The transformational role of GPU computing and deep learning in drug discovery. *Nature Machine Intelligence*, 4(3):211–221, March 2022. ISSN 2522-5839. doi: 10.1038/s42256-022-00463-x.

- [3] Priyanka Dixit and Sanjay Silakari. Deep Learning Algorithms for Cybersecurity Applications: A Technological and Status Review. *Computer Science Review*, 39:100317, February 2021. ISSN 15740137. doi: 10.1016/j.cosrev.2020.100317.
- [4] Marco Del Giudice. The Prediction-Explanation Fallacy: A Pervasive Problem in Scientific Applications of Machine Learning. preprint, PsyArXiv, December 2021. URL <https://osf.io/4vq8f>.
- [5] Gabrielle Ras, Ning Xie, Marcel Van Gerven, and Derek Doran. Explainable Deep Learning: A Field Guide for the Uninitiated. *Journal of Artificial Intelligence Research*, 73:329–397, January 2022. ISSN 1076-9757. doi: 10.1613/jair.1.13200.
- [6] Ramprasaath R. Selvaraju, Michael Cogswell, Abhishek Das, Ramakrishna Vedantam, Devi Parikh, and Dhruv Batra. Grad-CAM: Visual Explanations from Deep Networks via Gradient-based Localization. *International Journal of Computer Vision*, 128(2):336–359, February 2020. ISSN 0920-5691, 1573-1405. doi: 10.1007/s11263-019-01228-7.
- [7] Diogo V. Carvalho, Eduardo M. Pereira, and Jaime S. Cardoso. Machine Learning Interpretability: A Survey on Methods and Metrics. *Electronics*, 8(8):832, July 2019. ISSN 2079-9292. doi: 10.3390/electronics8080832. URL <https://www.mdpi.com/2079-9292/8/8/832>.
- [8] Scott M Lundberg and Su-In Lee. A unified approach to interpreting model predictions. In I. Guyon, U. V. Luxburg, S. Bengio, H. Wallach, R. Fergus, S. Vishwanathan, and R. Garnett, editors, *Advances in Neural Information Processing Systems 30*, pages 4765–4774. Curran Associates, Inc., 2017.
- [9] Leo Breiman. Statistical Modeling: The Two Cultures (with comments and a rejoinder by the author). *Statistical Science*, 16(3), August 2001. ISSN 0883-4237. doi: 10.1214/ss/1009213726.
- [10] Robert Anderson. The Rashomon Effect and Communication. *Canadian Journal of Communication*, 41(2):249–270, May 2016. ISSN 0705-3657, 1499-6642. doi: 10.22230/cjc.2016v41n2a3068. URL <https://cjc.utpjournals.press/doi/10.22230/cjc.2016v41n2a3068>.
- [11] Cynthia Rudin, Chaofan Chen, Zhi Chen, Haiyang Huang, Lesia Semenova, and Chudi Zhong. Interpretable Machine Learning: Fundamental Principles and 10 Grand Challenges, July 2021. URL <http://arxiv.org/abs/2103.11251>. arXiv:2103.11251 [cs, stat].
- [12] Charles T. Marx, Flavio du Pin Calmon, and Berk Ustun. Predictive Multiplicity in Classification, September 2020. URL <http://arxiv.org/abs/1909.06677>. arXiv:1909.06677 [cs, stat].
- [13] Damien Teney, Maxime Peyrard, and Ehsan Abbasnejad. Predicting is not Understanding: Recognizing and Addressing Underspecification in Machine Learning, July 2022. URL <http://arxiv.org/abs/2207.02598>. arXiv:2207.02598 [cs].
- [14] Chirag Agarwal, Satyapriya Krishna, Eshika Saxena, Martin Pawelczyk, Nari Johnson, Isha Puri, Marinka Zitnik, and Himabindu Lakkaraju. OpenXAI: Towards a Transparent Evaluation of Model Explanations, January 2023.
- [15] Ashish Bhardwaj. Framingham heart study dataset.
- [16] Hans Hofmann. Statlog (German Credit Data), 1994.
- [17] Jack W. Smith, J.E. Everhart, W.C. Dickson, W.C. Knowler, and R.S. Johannes. Using the ADAP Learning Algorithm to Forecast the Onset of Diabetes Mellitus. pages 261–265, 1988.
- [18] Kareem L. Jordan and Tina L. Freiburger. The Effect of Race/Ethnicity on Sentencing: Examining Sentence Type, Jail Length, and Prison Length. *Journal of Ethnicity in Criminal Justice*, 13(3):179–196, July 2015. ISSN 1537-7938, 1537-7946. doi: 10.1080/15377938.2014.984045.
- [19] Moez Ali. *PyCaret: An open source, low-code machine learning library in Python*, April 2020. URL <https://www.pycaret.org>. PyCaret version 1.0.
- [20] Jacob Cohen. A Coefficient of Agreement for Nominal Scales. *Educational and Psychological Measurement*, 20(1):37–46, April 1960. ISSN 0013-1644, 1552-3888. doi: 10.1177/001316446002000104.
- [21] Scott Lundberg and Su-In Lee. A Unified Approach to Interpreting Model Predictions. *arXiv:1705.07874 [cs, stat]*, November 2017.
- [22] Pål Vegard Johnsen, Inga Strümke, Mette Langaas, Andrew Thomas DeWan, and Signe Riemer-Sørensen. Inferring feature importance with uncertainties with application to large genotype data. *PLoS Computational Biology*, 19(3):e1010963, March 2023. ISSN 1553-7358. doi: 10.1371/journal.pcbi.1010963.
- [23] Andreas Messalas, Yiannis Kanellopoulos, and Christos Makris. Model-Agnostic Interpretability with Shapley Values. In *2019 10th International Conference on Information, Intelligence, Systems and Applications (IISA)*, pages 1–7, PATRAS, Greece, July 2019. IEEE. ISBN 978-1-72814-959-2. doi: 10.1109/IISA.2019.8900669.
- [24] Yosef Hochberg. A sharper Bonferroni procedure for multiple tests of significance. page 3, 1988.
- [25] Yoav Wald, Amir Feder, Daniel Greenfeld, and Uri Shalit. On Calibration and Out-of-domain Generalization, January 2022.
- [26] Behnam Neyshabur, Hanie Sedghi, and Chiyuan Zhang. What is being transferred in transfer learning?, January 2021.
- [27] Dr. Mehmet Cem Çatalbaş. An Investigation into the Relationship between Curse of Dimensionality and Dunning-Kruger Effect. *Sakarya University*

Journal of Computer and Information Sciences, 3
(2):121–130, August 2020. ISSN 2636-8129. doi:
10.35377/saucis.03.02.727032.